CROATICA CHEMICA ACTA
CCACAA **76** (1) 37–48 (2003)

ISSN-0011-1643
CCA-2850
Original Scientific Paper

A Theoretical and Experimental Study of a Two-step Quasireversible Surface Redox Reaction by Square-wave Voltammetry

Valentin Mirčeski* and Rubin Gulaboski**

Ernst-Moritz-Arndt-Universität Greifswald, Institut für Chemie und Biochemie, Soldtmannstraße 23, D-17489 Greifswald, Germany

RECEIVED MAY 13, 2002; REVISED SEPTEMBER 23, 2002; ACCEPTED OCTOBER 4, 2002

Key words
square-wave voltammetry
EE reaction
simulations
surface reactions
azo-dyes
Sudan-III

An extended theoretical treatment of a two-step surface redox reaction under the conditions of square-wave voltammetry (SWV) is presented. The theoretical model is applicable to any reversibility of both redox steps of the EE reaction. The integral equations representing this theoretical model were solved numerically. The apparent reversibility of the redox steps depends on two dimensionless kinetic parameters, κ_1 and κ_2, defined as $\kappa_1 = k_{s,1}/f$ and $\kappa_2 = k_{s,2}/f$, where $k_{s,1}$ and $k_{s,2}$ are the standard rate constants of the first and second redox steps, respectively, and f is the excitation signal frequency. The response consists of either a single or two separate SW peaks, depending mainly on the difference between the formal potentials of the first and second redox steps as well as on the ratio of the kinetic parameters κ_1/κ_2. The effect of the electron transfer coefficients of both redox steps is also discussed. A part of the theoretical results are qualitatively illustrated by SW voltamograms of the azo-dye Sudan-III.

INTRODUCTION

Electrode transformations of many electroactive organic compounds, as well as of some metal ions, occurring at the electrode surface are frequently accompanied by adsorption phenomena.[1–17] In recent decades, numerous studies have demonstrated that square-wave voltammetry (SWV) is an exceptionally convenient technique for investigating the adsorption-coupled electrode reactions.[7–10,12,17] Characterised by unique advantages, such as a high scan rate, large signal amplitude, effective ability to discriminate against the charging current, as well as the ability to provide an insight into both half-reactions of the redox process, SWV is one of the most advanced members in the family of the pulse voltammetric techniques.[17–26]

The theory of SWV-related redox mechanisms accompanied by adsorption phenomena is still in progress. Recently, attention has been paid to the study of simple diffusionless surface redox processes in which both components of the redox couple are immobilised on the electrode surface.[9,10,22,25,26] In our recent study,[10] it was shown that SWV enabled both thermodynamic and kinetic characterisation of the surface reaction by a simple and fast procedure. On the other hand, surface-confined electrode processes are of considerable importance since they are frequently encountered in redox polymer films, self-assembled structures populated with redox sites, and

* On leave from: Department of Chemistry, Faculty of Natural Sciences and Mathematics, »Sv. Kiril i Metodij« University, P.O. Box 162, 1000 Skopje, Republic of Macedonia.
** Author to whom correspondence should be addressed. (E-mail: RubinGulaboski@excite.com)

simple adsorbates. Thus, it is of keen interest to extend the applicability of SWV to more complex surface electrode pathways.

Recently, Armstrong *et al.*[27–31] established a new field of application of surface redox reactions. In the so-called protein film voltammetry, these authors demonstrated how to deduce valuable data about the physiological activity of proteins by studying their surface electrode reactions. The principle of protein film voltammetry is that the protein sample is confined to the electrode surface, ideally as a homogeneous population in a monolayer coverage, affording opportunities for a detailed study of electron transfer and coupled reactions in proteins.

Although electrode reactions of many adsorbates occur in one step, cases exist where two or more redox steps have been observed, such as azo-dyes,[11–12] and aromatic carbonyl compounds.[14–15] For these compounds, the product of the initial reduction undergoes further electrode transformation at either a more negative or the same potential as for the initial reduction step. This type of electrode reaction is designated as EE mechanism.

The theory of an electrode process consisting of two successive surface redox reactions under the conditions of linear scan voltammetry and simple dc-polarography, was developed by Laviron *et al.*[16] The theoretical treatment of the surface EE electrode reaction under the conditions of SWV was recently initiated by O'Dea *et al.*[12] In their study, the theoretical consideration was restricted to the surface EE mechanism in which the first step was quasireversible and the second one totally irreversible.

In this study, we have extended the theoretical treatment of the EE electrode reaction to the case in which both redox reactions are chemically reversible and characterised by different standard rate constants, as well as different electron transfer coefficients. The mathematical solutions are represented as integral equations, and thus they can be applied to any chronoamperometric technique. The numerical solutions are adapted to the conditions of SWV. The aim of the work is to study the relationships between the properties of the SWV response and the kinetic and thermodynamic properties of the surface EE electrode reactions. It is demonstrated that under certain conditions SW enables access to the kinetics of both redox steps utilising the method of the »quasireversible maximum«. The origin of this phenomenon is explained by the theoretical treatment of the simple surface redox reaction under chronoamperometric conditions. The ability of SW to discriminate against the charging current for surface redox reactions is also briefly examined.

A part of the numerical results are qualitatively illustrated by the experimental SW voltamograms of Sudan-III (1-[4-(phenylazo)phenylazo]-2-naphtol). Sudan-III is a well-known bis-azo dye,[11] which undergoes a two-step electrochemical reduction in both non-aqueous and aqueous media. The comparison with the SW voltammetric behaviour of Sudan-III serves only to confirm the validity of the theoretical models and numerically simulated data.

EXPERIMENTAL

Sudan-III (1-[4-(phenylazo)phenylazo]-2-naphtol) (Aldrich Co.), borate buffer with pH = 10 (Fluka) and ethanol (Kemika, Zagreb) were used as received. Water was doubly distilled. A stock solution of Sudan-III, concentration 0.01 mol dm^{-3}, was prepared by dissolving it in absolute ethanol. 0.1 mol dm^{-3} borate buffers with pH = 10 values were used as supporting electrolytes.

All measurements were performed at room temperature. Extra pure nitrogen was purged through the solutions for 8 minutes prior to the first measurement and a nitrogen blanket was maintained thereafter.

All voltamograms were recorded using a μAutolab (ECO Chemie, Utrecht, Netherlands) which was connected to the static mercury drop electrode (SMDE), Model 303A, from Princeton Applied Research. A platinum wire was used as an auxiliary electrode and Ag | AgCl | KCl (3 mol dm^{-3}) as reference electrode.

MATHEMATICAL MODEL

Consider the surface redox reaction in which species A converts electrochemically to B, while B reduces concurrently to the final product C. Both steps are chemically reversible first order redox reactions. Omitting the charge of the species, the electrode mechanism can be represented by the following Scheme I:

$$A_{(ads)} + ne^- \rightleftharpoons B_{(ads)} + ne^- \rightleftharpoons C_{(ads)}$$

Scheme I.

All participants in the above mechanism are chemically stable species and are confined firmly to the working electrode surface. In the absence of lateral interactions, the boundary value problem is defined as:

$$\frac{d\Gamma(A)}{dt} = -\frac{I_1}{n_1 FS} \quad (1)$$

$$\frac{d\Gamma(B)}{dt} = \frac{I_1}{n_1 FS} - \frac{I_2}{n_2 FS} \quad (2)$$

$$\frac{d\Gamma(C)}{dt} = \frac{I_2}{n_2 FS} \quad (3)$$

(a) $t = 0$, $\Gamma(A) = \Gamma^*$, $\Gamma(B) = \Gamma(C) = 0$

(b) $t > 0$, $\Gamma(A) + \Gamma(B) + \Gamma(C) = \Gamma^*$

Γ(A), Γ(B) and Γ(C) are surface concentrations of electroactive species A, B and C, respectively, Γ^* is the total surface concentration of adsorbates, and n_1 and n_2 are the number of electrons exchanged in the first and second electrode steps, respectively, while *I/S* is the current density. Subscripts 1 and 2 refer to the first (A → B) and second (B → C) redox steps, respectively. The other symbols have their usual meaning.

The solutions of the above equations, which represent the variation of surface concentrations with time, are:

$$\Gamma(\mathrm{A}) = \Gamma^* - \int_0^t \frac{I_1(\tau)}{n_1 FS}\,\mathrm{d}\tau \tag{4}$$

$$\Gamma(\mathrm{B}) = \int_0^t \frac{I_1(\tau)}{n_1 FS}\,\mathrm{d}\tau - \int_0^t \frac{I_2(\tau)}{n_2 FS}\,\mathrm{d}\tau \tag{5}$$

$$\Gamma(\mathrm{C}) = \int_0^t \frac{I_2(\tau)}{n_2 FS}\,\mathrm{d}\tau \tag{6}$$

In addition, the following conditions hold at the electrode surface:

$$\frac{I_1}{n_1 FS} = k_{\mathrm{s},1}\,\exp(-\alpha_1\varphi_1)[\Gamma(\mathrm{A}) - \exp(\varphi_1)\Gamma(\mathrm{B})] \tag{7}$$

$$\frac{I_2}{n_2 FS} = k_{\mathrm{s},2}\,\exp(-\alpha_2\varphi_2)[\Gamma(\mathrm{B}) - \exp(\varphi_2)\Gamma(\mathrm{C})] \tag{8}$$

Here, $k_{\mathrm{s},1}$ and $k_{\mathrm{s},2}$ are the standard rate constants expressed in units of s^{-1}, and α_1 and α_2 are electron transfer coefficients of the first and second redox steps, respectively. φ_1 and φ_2 are dimensionless potentials, defined as $\varphi_1 = \dfrac{n_1F(E-E_{\mathrm{f,A/B}})}{RT}$ and $\varphi_2 = \dfrac{n_2F(E-E_{\mathrm{f,B/C}})}{RT}$, where $E_{\mathrm{f,A/B}}$ and $E_{\mathrm{f,B/C}}$ are the formal redox potentials of the first and second steps, respectively.

Substituting eqs. (4) and (5) into (7), and (5) and (6) into (8), one obtains a set of integral equations, which can be regarded as a mathematical representation of the surface EE electrode mechanism under chronoamperometric conditions:

$$\frac{I_1}{n_1 FS} = k_{\mathrm{s},1}\,\exp(-\alpha_1\varphi_1)\cdot$$

$$\left[\Gamma^* - \int_0^t \frac{I_1(\tau)}{n_1 FS}\,\mathrm{d}\tau - \exp(\varphi_1)\left(\int_0^t \frac{I_1(\tau)}{n_1 FS}\,\mathrm{d}\tau - \int_0^t \frac{I_2(\tau)}{n_2 FS}\,\mathrm{d}\tau\right)\right] \tag{9}$$

$$\frac{I_2}{n_2 FS} = k_{\mathrm{s},2}\,\exp(-\alpha_2\varphi_2)\cdot$$

$$\left[\int_0^t \frac{I_1(\tau)}{n_1 FS}\,\mathrm{d}\tau - \int_0^t \frac{I_2(\tau)}{n_2 FS}\,\mathrm{d}\tau - \exp(\varphi_2)\int_0^t \frac{I_2(\tau)}{n_2 FS}\,\mathrm{d}\tau\right] \tag{10}$$

For numerical simulations, both variables, current *I* and time *t*, were incremented. To each time $t = m\,d$, where *d* is the time increment, a certain current I_m was ascribed. Time increment is defined as $d = 1/(50\,f)$ (= $0.02/f$), which means that each potential pulse of the excitation signal is divided into 25 equal time increments. The numerical solutions of integral equations (9) and (10), obtained by the method of Nicholson and Olmstead,[32] are:

$$\Psi_{1,m} = \kappa_1\,\exp(-\alpha_1\varphi_{1,m})\cdot$$

$$\frac{\left[1-0.02(1+\exp(\varphi_{1,m}))\sum_{j=1}^{m-1}\Psi_{1,j} + 0.02\exp(\varphi_{1,m})(\Psi_{2,m} + \sum_{j=1}^{m-1}\Psi_{2,j})\right]}{1+0.02\kappa_1\exp(-\alpha_1\varphi_{1,m})(1+\exp(\varphi_{1,m}))} \tag{11}$$

$$\Psi_{2,m} = \frac{0.02\kappa_2\,\exp(-\alpha_2\varphi_{2,m})\left[\Psi_{1,m} + \sum_{j=1}^{m-1}\Psi_{1,j} - (1+\exp(\varphi_{2,m}))\sum_{j=1}^{m-1}\Psi_{2,j}\right]}{1+0.02\kappa_2\,\exp(-\alpha_2\varphi_{2,m})(1+\exp(\varphi_{2,m}))} \tag{12}$$

Here, κ_1 and κ_2 are kinetic parameters defined as $\kappa_1 = k_{\mathrm{s},1}/f$, and $\kappa_2 = k_{\mathrm{s},2}/f$, where *f* is the SW signal frequency, and $\Psi_1 = \dfrac{I_1}{n_1FSf\Gamma^*}$ and $\Psi_2 = \dfrac{I_2}{n_2FSf\Gamma^*}$ are the dimensionless currents of the first and second redox steps, respectively. The dimensionless current for the overall two-step process is defined as: $\Psi = \Psi_1 + \Psi_2$.

The square-wave signal is a train of cathodic and anodic pulses superimposed on a staircase potential ramp. The height of each cathodic and anodic pulse is equal and designated as the square-wave amplitude E_{sw}. Additionally, the SW signal is characterised by the staircase potential increment d*E* and frequency *f* of the pulses.[18]

For comparison, a simple one-step surface redox reaction was considered:

$$\mathrm{A}_{(\mathrm{ads})} + n\mathrm{e}^- \rightleftharpoons \mathrm{B}_{(\mathrm{ads})}$$

Scheme II.

The procedure for numerical simulations of this reaction is described elsewhere.[10]

THEORETICAL RESULTS

The dimensionless SW voltamograms are current-potential bell-shaped curves defined by the peak potential E_{p}, peak current $\Delta\Psi_{\mathrm{p}}$ and half-peak width $w_{1/2}$. These properties of the voltammetric response to the current redox mechanism are functions of the following parameters:

number of exchanged electrons n_1 and n_2, formal redox potentials $E_{f,A/B}$ and $E_{f,B/C}$, standard rate constants $k_{s,1}$ and $k_{s,2}$, electron transfer coefficients α_1 and α_2, temperature T, and the excitement signal parameters. Moreover, the responses were analysed with respect to a new thermodynamic parameter defined as the difference between the formal redox potentials $\Delta E_f = E_{f,B/C} - E_{f,A/B}$. This parameter predominantly determines the overall shape of the voltammetric response. If the formal potential difference is $\Delta E_f < 0$, the second redox step occurs at a more negative potential than the first one, which is the first prerequisite for the appearance of two separate SW peaks. For $\Delta E_f \geq 0$, only a single peak arises, since the second redox step occurs at the same or more positive potential than the first one. On the other hand, the reversibility of both redox steps is determined mainly by the kinetic parameters κ_1 and κ_2, and, to some extent, by the electron transfer coefficients α_1 and α_2.

Figure 1 shows theoretical SW voltamograms simulated for $\kappa_1 = \kappa_2 = 1$ and several values for ΔE_f. For $\Delta E_f \geq$ –50 mV, the response consists of a single SW peak (curves A and B in Figure 1). Its position, height and half-peak width are strongly dependent on the values of ΔE_f. Increasing the value of ΔE_f from –50 to 0 mV, the peak potential shifts in a positive direction. The increase of the standard potential difference corresponds to the conditions when the second redox process gradually approaches the first one, which occurs at slightly more positive potentials. For these reasons, the peak current of the single SW peak increases, while the half-peak width decreases. When the second redox step proceeds at either equal or more positive potentials than the first one, the standard potential difference ΔE_f no longer affects the properties of the response.

For ΔE_f = –100 mV, the response consists of two partly overlapped SW peaks (curve C in Figure 1). Overlapping of the SW peaks is present permanently within the interval $-150 \text{ mV} \leq \Delta E_f \leq -100$ mV. If the second redox step occurs at potentials that are 150 mV more negative than the first process, then both redox processes are isolated effectively and two well-separated SW peaks are observed.

Therefore, with respect to the formal potential difference ΔE_f, three distinct cases may be considered:

Case A. The second redox step occurs at potentials that are at least 150 mV more negative than the potential of the first step, or $\Delta E_f \leq -150$ mV.

Case B. The second redox step occurs at either equal or more positive potentials than the first step, $\Delta E_f \geq 0$ mV.

Case C. An intermediate case where $-150 \text{ mV} < \Delta E_f < 0$ mV.

Interestingly, similar intervals have been observed in the study of the diffusion EE mechanism by cyclic voltammetry.[33] In that study, two separate CV waves are observed for $\Delta E_f < -180$ mV. In the intermediate region, $-100 \text{ mV} < \Delta E_f < 0$ mV, the two waves are merged in a single broad wave, whereas for $\Delta E_f > 180$ mV (*i.e.,* the second step is much easier than the first), a single wave characteristic of a direct $2e^-$ reduction is observed.

Case A ($\Delta E_f \leq -150$ mV)

If $\Delta E_f \leq -150$ mV, both redox processes of the surface EE mechanism are isolated effectively, acting virtually as an independent surface redox reactions. In this situation, thermodynamic conditions for the electrochemical conversion of the intermediate B to the final product C are fulfilled only at potentials that are much more negative relative to the first electrochemical transformation. The response consists of two well-developed SW peaks, with a potential separation depending on the standard potential difference ΔE_f and particular values of the ki-

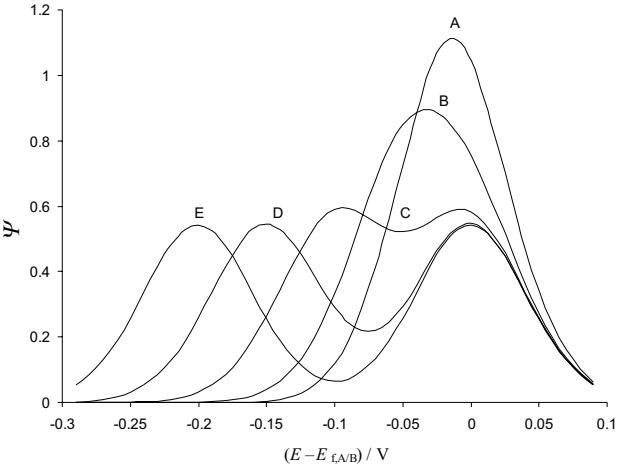

Figure 1. SW voltamograms of a surface EE reaction simulated for a formal potential difference of ΔE_f = 0 (A), –50 (B), –100 (C), –150 (D) and –200 mV (E). The other conditions of the simulations were: $\alpha_1 = \alpha_2 = 0.5$, $n_1 = n_2 = 1$, $\kappa_1 = \kappa_2 = 1$, potential step dE = 10 mV and square-wave amplitude E_{sw} = 30 mV.

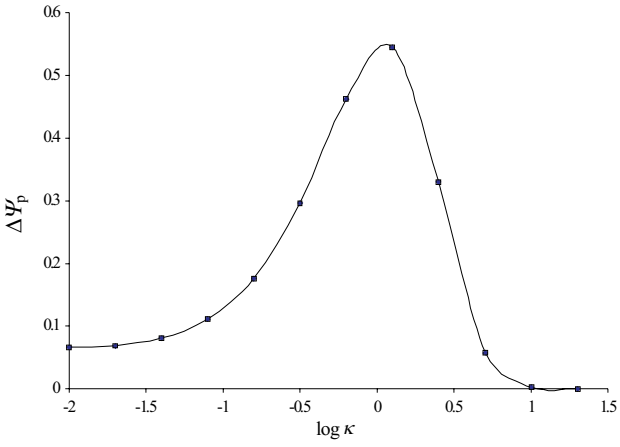

Figure 2. (case A) The dependence of the dimensionless peak current $\Delta\Psi_p$ on the logarithm of the kinetic parameter κ, simulated for the formal potential difference of ΔE_f = –200 mV. This dependence applies equivalently to both redox steps of the EE reaction. All the other conditions of the simulations were the same as in Figure 1.

netic parameters κ_1 and κ_2. On the other hand, the height of the SW peaks is affected primarily by kinetic parameters, and to some extent by the electron transfer coefficients α_1 and α_2.

The dependence of the dimensionless peak current $\Delta\Psi_p$ on the kinetic parameter κ is illustrated in Figure 2. It should be stressed that this dependence is equally valid for both SW peaks. Being parabolically dependent on the kinetic parameter κ, the peak current dramatically increases within the quasireversible region ($-1 < \log\kappa < 1$). This is a well-known property of the surface redox reaction named »quasireversible maximum«.[4,5,7,8,22–26]

The position of the quasireversible maximum is associated with a certain critical value of the kinetic argument κ_{max}, which depends on the electron transfer coefficient α and the signal amplitude E_{sw}. The critical values of κ_{max} have already been calculated for series of α and E_{sw}.[7,8] In the real experiment, the quasireversible maximum could be demonstrated by varying the signal frequency. Plotting the ratio of the real peak current and the corresponding frequency $\Delta I_p/f$ *versus* the inverse signal frequency $1/f$, one could reconstruct the theoretical dependence depicted in Figure 2. If the critical frequency associated with the quasireversible maximum f_{max} is obtained experimentally and if the critical value of the kinetic parameter κ_{max} is calculated theoretically, the standard rate constant of the surface redox reaction could be estimated using the following simple relation: $k_s = \kappa_{max} f_{max}$.

Apparently, the quasireversible maximum is an important property, which enables estimation of the standard rate constant by a simple and fast experimental procedure. The quasireversible maximum could be employed independently for both SW peaks, enabling assessment of the redox kinetics of both steps of the surface EE mechanism. If the electrode mechanism is investigated under the conditions of cyclic voltammetry, the method of Laviron[34] can be applied for same purposes. The method requires an extrapolation of the data, which generally involves a larger error in the estimation of the standard rate constant than the method of »quasireversible maximum«. Moreover, the CV cannot resolve contributions of the charging and faradic components in the overall voltammetric response, which appears to be the major disadvantage of this technique. As explained in the Appendix, square-wave voltammetry avoids efficiently the contribution of the charging current, providing exclusively data about the redox transformation of the electroactive film confined to the electrode surface.

The theoretical response of the surface EE reaction gains an interesting shape for the large signal amplitude and height reversibility of the redox steps of the EE reaction. Figure 3 shows the theoretical response calculated for $\Delta E_f = -200$ mV, $E_{sw} = 50$ mV and $\kappa_1 = \kappa_2 = 5$. For such conditions, the SW response of the surface EE

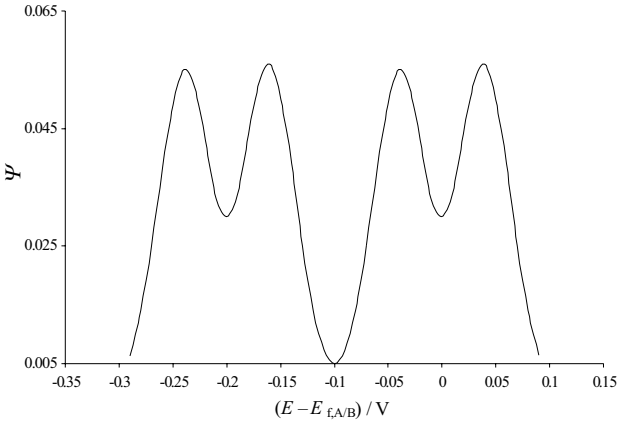

Figure 3. (case A) Theoretical SW voltamograms of the EE reaction simulated for $\kappa_1 = \kappa_2 = 5$, $\Delta E_f = -200$ mV and $E_{sw} = 50$ mV. All other conditions of the simulations are the same as in the caption to Figure 1.

reaction consists of four SW peaks as a consequence of the splitting of both SW peaks. It was recently shown[10] that, under certain experimental conditions, the response of a fast and chemically reversible surface redox reaction splits into two SW peaks as a result of the large separation between the cathodic and anodic components of the SW voltammetric response. The potential separation between the split peaks is sensitive to the redox kinetics, and therefore it may additionally serve for estimating the standard rate constants of both redox steps following the procedure elaborated in our previous communication.[10]

According to the methodology developed (Ref. 10), the kinetics of the fast surface redox reaction can be studied by varying the signal amplitude at a low signal frequency. In cyclic voltammetry, the accessibility of the kinetics of the fast surface redox reaction is possible only at extremely high scan rates. Under such conditions, the quality of the CV data is severely affected by the contributions of the charging current and ohmic drop, since both effects increase proportionally to the scan rate.

In conclusion, when both redox steps of the EE reaction are effectively isolated ($\Delta E_f \leq -150$ mV), the properties of each SW peak are quite close to that of the corresponding simple one-step surface reaction. Consequently, the previously described methods of a »quasireversible maximum« [7,8] and »split SW peaks«[10] for redox kinetic measurements of the surface redox reactions are fully applicable to each step of the EE reaction.

Case B ($\Delta E_f \geq 0$ mV)

This is the case in which the thermodynamic conditions for the electrochemical conversion of intermediate B to the final product C are fulfilled immediately after creation of B *via* the first redox reaction. This is an exceptionally important case, since it can be regarded as a possible pathway of many two-electron quasireversible

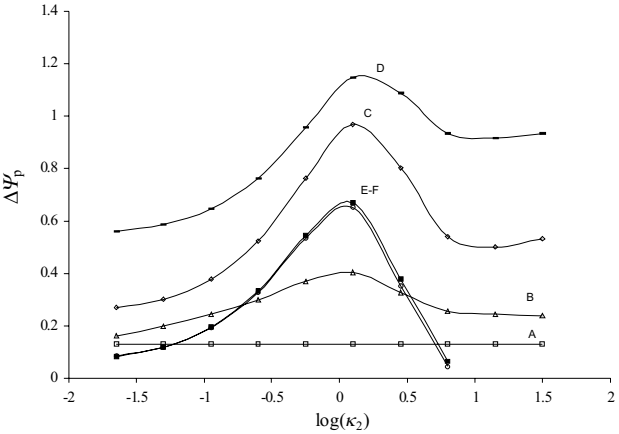

Figure 4. (case B) The dependence of the dimensionless peak current $\Delta\Psi_p$ on the kinetic parameter κ_2 for the formal potential difference of $\Delta E_f = 0$ mV. The values of the kinetic parameter κ_1 are: $\log(\kappa_1) = -3.5$ (A), –1 (B), 0 (C), 0.48 (D), 0.90 (E), and 1 (F). All other conditions of the simulations were the same as in Figure 1.

surface redox reactions, which were already experimentally studied.[11–15]

The response consists of a single SW peak, whose position is independent of the formal potential difference ΔE_f. The properties of the voltammetric response are affected predominantly by the kinetic parameters κ_1 and κ_2, and electron transfer coefficients α_1 and α_2.

Figure 4 shows the effect of the kinetic parameter κ_2 on the dimensionless peak currents for several constant values of the kinetic parameter κ_1. This theoretical analysis illustrates the comparison of different EE reactions characterised by the same rate of the first redox step and different rates of the second one. For $\log(\kappa_1) = -3.5$ (curve A in Figure 4), the kinetic parameter of the second redox step κ_2 exhibits no influence on the peak currents, whereas for $\log(\kappa_1) = -1$ (curve B in Figure 4), the kinetic parameter κ_2 exhibits only a slight influence on the peak currents. In the interval $\log(\kappa_1) \leq -3.5$, the limiting conditions are reached and the kinetics of the overall EE reaction is determined solely by the kinetics of the first redox step, which is slow and electrochemically irreversible.

The second limiting situation appears when the kinetic parameter of the first redox step is within the reversible region ($\log(\kappa_1) > 0.8$). For these conditions, the kinetics of the overall process is solely determined by the kinetics of the second step (curves E and F in Figure 4). In the intermediate case, $-3.5 \leq \log(\kappa_1) \leq 0.8$, the kinetics of the surface EE reaction is a complex function of the kinetics of both redox steps (curves C and D in Figure 4) and the peak currents depend on both kinetic parameters, κ_1 and κ_2.

The foregoing theoretical analysis serves to reveal the conditions under which the EE reaction is controlled by the kinetics of a single redox step. However, it should be emphasised that this theoretical analysis does not correspond to the real experimental case in which a single reaction is studied. In the experiment, it is not possible to vary a single kinetic parameter independently. Both kinetic parameters κ_1 and κ_2 can be simultaneously varied by changing the SW frequency from a certain minimal f_{min} to a maximal value f_{max}. Thus, the overall process is controlled by the kinetics of the first redox step if the condition $\log(k_{s,1}/f_{min}) \leq -3.5$ is fulfilled. Whereas, the overall process is controlled solely by the kinetics of the second redox step for $\log(k_{s,1}/f_{max}) \geq 0.8$.

As expected, when both steps of the EE reaction are quasireversible, the complexity of the system increases considerably. Processing numerous simulated voltamograms, an attempt was made to elucidate the specific properties of the system, and to establish criteria, if possible, of distinguishing the EE mechanism from the simple one-step surface reaction. For these purposes, a comparative analysis of the two-electron EE reaction (Scheme I) and two-electron one-step (Scheme II) surface redox reaction was made.

In Figure 5, the theoretical responses of these two different redox reactions, simulated under identical conditions, are presented. Each redox step is associated with identical kinetic parameters: $\kappa = 2$ and $\alpha = 0.5$. Comparing the net-SW responses of reactions (I) and (II) (compare curve 3 in Figures 5A and 5B), it is obvious that the two-electron EE reaction produces a higher response than the corresponding two-electron one-step surface reaction. Interestingly, the response of the second step of the EE reaction (curve 2 in Figure 5A) is higher than the response of the first step (curve 1 in Figure 5A) although both processes proceed at an equal rate.

By studying the quasireversible maximum, it was well-understood that the response of the surface redox reaction increases dramatically within the quasireversible region.[7] Under these conditions, the enhancement of the response is mainly due to kinetic reasons, *i.e.,* synchronisation of the rate of the redox reaction with the frequency of the excitation signal. The amount of the measured current for a quasireversible redox reaction does not depend considerably on the number of exchanged electrons. Therefore, to some extent, it is understandable why the two successive one-electron quasireversible transformations in the EE reaction produce a larger current than the one-step two-electron transformation in the case of reaction (II).

However, it is still not clear why the response of the second step of the EE reaction is higher than the first one, although both steps proceed at an equal rate. It appears that a certain pseudo-catalytic phenomenon takes place for the second redox step of the EE reaction. In the course of the anodic pulses of the SW excitation signal, the final product C can be reoxidised to the intermediate B, as well as to the initial reactant A, since both processes occur at the same potential. As a consequence, the intermediate B, acting as a reactant for the second re-

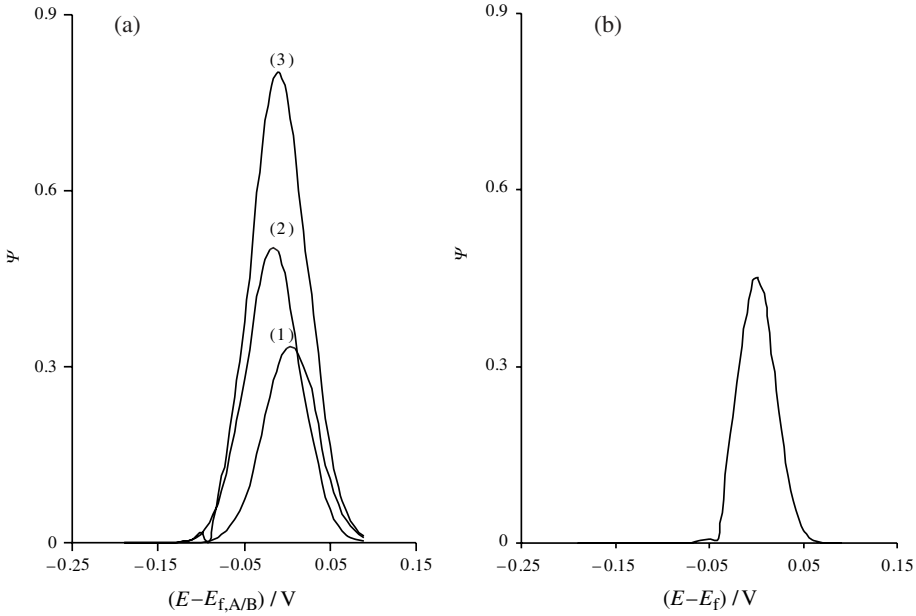

Figure 5. (case B) (a): The net-SW response of the first (curve 1), second (curve 2), and the overall (curve 3) redox step of the EE mechanism simulated for $\kappa_1 = \kappa_2 = 2$, and $\Delta E_f = 0$ mV, $n_1 = n_2 = 1$ and $\alpha_1 = \alpha_2 = 0.5$. (b) The net-SW response of a simple two-electron one-step surface redox reaction simulated for $\kappa = 2$ and $\alpha = 0.5$. The other conditions of the simulations valid for both reactions were: square-wave amplitude $E_{sw} = 30$ mV and potential step $dE = 10$ mV.

dox step, is regenerated permanently by both the anodic oxidation of the final product C and the cathodic reduction of the initial reactant A. This gives rise to pronounced currents in the second redox step, which contribute considerably to the overall response of the EE reaction.

Although the overall behaviour of the net-SW response of the reaction mechanisms (I) and (II) is rather similar, it is of particular importance to emphasise that the half-peak width of the net-SW response of the EE reaction (curve 3 in Figure 5A) is considerably different from that of the one-step surface redox reaction (Figure 5B). Figure 6 shows the variation of the half-peak width with the logarithm of the kinetic parameter κ for both reactions. The half-peak widths decrease with the kinetic parameter for both reactions. However, the values for the EE reaction are on average 40 mV higher than that of the one-step two-electron reaction.

The variation of the electron transfer coefficients α_1 and α_2 over the interval from 0.3 to 0.8 exhibits a slight influence upon the peak currents, whereas the peak potential and half-peak width are independent of transfer coefficients. The peak current of the overall process depends parabolically on α, with a maximum positioned at 0.5, which holds for both α_1 and α_2.

To conclude, in the experimental reality, the analysis of the response by varying the signal frequency is strongly recommended. Measuring the half-peak width of the single SW peak and plotting it *versus* the signal frequency, one obtains a dependency corresponding one of those presented in Figure 6. This analysis should provide information whether the reaction studied proceeds as an EE, or a simple one-step surface redox process. At the same time, analysing the peak current as a function of the signal frequency, one can obtain parabolic dependencies, as presented in Figure 4. The curves in Fig-

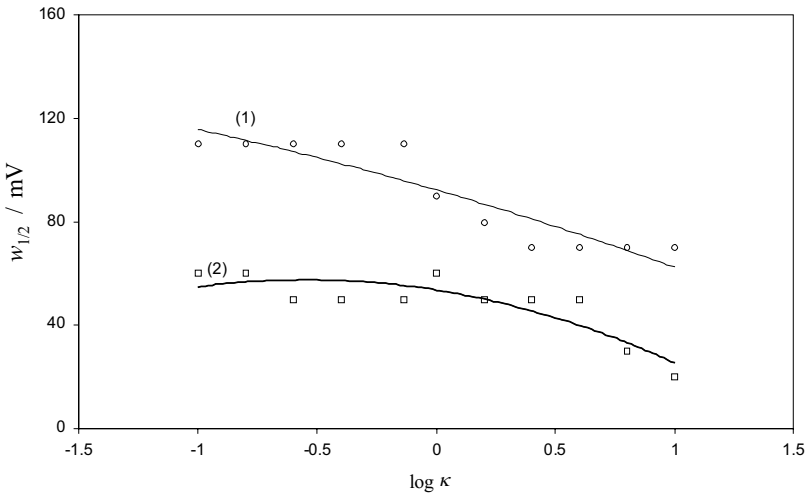

Figure 6. (case B) The dependence of the half-peak width for the two-electron EE reaction (curve 1) and the two-electron one-step surface reaction (curve 2) on the kinetic parameter. The conditions of the simulations for the EE and simple surface reactions were the same as in Figure 5(a) and (b), respectively.

ure 4 represent the quasireversible maxima for the EE reaction. However, if the redox reaction proceeds under limiting conditions, *i.e.*, it is controlled by the kinetics of the single step, the quasireversible maximum can provide kinetic information for the rate-controlling step. Otherwise, when both redox steps contribute to the kinetics of the overall process, the quasireversible maximum does not allow extraction of accurate kinetic data.

*Case C (–150 mV ≤ Δ*E*$_f$ ≤ 0 mV)*

In this case, the response of the EE reaction consists of either a single peak or two overlapped SW peaks, depending on the kinetic parameters κ_1 and κ_2 as well as on the formal potential difference ΔE_f. When two SW peaks are observed, their peak heights are determined mainly by the magnitudes of the kinetic parameters κ_1 and κ_2, and transfer coefficients α_1 and α_2, whereas their potential separation depends on the formal potential difference ΔE_f and the ratio κ_1/κ_2.

Figure 7 represents a variety of SWV responses simulated for a constant standard potential difference of ΔE_f = –100 mV and a series of different ratios κ_1/κ_2. For $\kappa_1/\kappa_2 \leq 0.2$, a single SW peak is observed (Figure 7, curve A). Increasing the ratio κ_1/κ_2 causes the response to split into two peaks. For κ_1/κ_2 = 0.79, the potential separation between the overlapped SW peaks is 70 mV (Figure 7, curve B). In general, the potential separation increases in proportion to κ_1/κ_2. It is important to note that for κ_1/κ_2 = 50, the potential separation is 180 mV, which is larger than the actual formal potential difference ΔE_f (see curve C in Figure 7).

A more detailled analysis of the influence of the ratio κ_1/κ_2 on the potential separation for various values of ΔE_f is represented in Figure 8. Under certain conditions, *e.g.* $\kappa_1/\kappa_2 > 200$, two separate SW peaks can be observed, even for ΔE_f = 0 mV. It is worth noting that if the potential separation between the SW peaks is greater than 75 mV, the kinetics of both redox steps may be independently inspected applying the method of »quasireversible maximum«, or some other method for kinetic measurements.

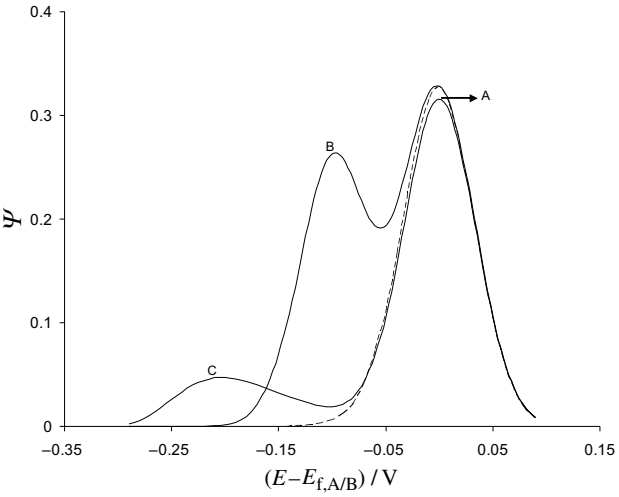

Figure 7. (case C) Theoretical SW voltamograms of the EE reaction simulated for a formal potential difference of ΔE_f = –100 mV. The ratio of the kinetic parameters is κ_1/κ_2= 0.2 (A), 0.7 (B) and 50 (C). All other conditions of the simulations are the same as in the caption to Figure 1.

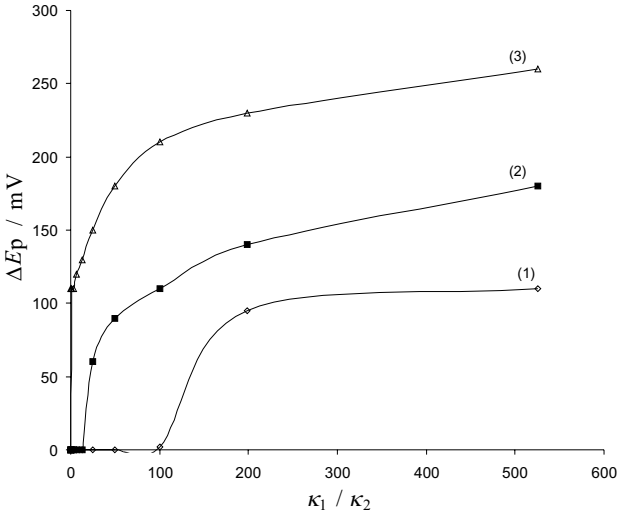

Figure 8. (case C) The dependence of the peak potential separation ΔE_p between the SWV peaks of the EE reaction on the ratio κ_1/κ_2. The formal potential difference is: ΔE_f = 0 (1), 50 (2) and 100 mV (3). All other conditions of the simulations are the same as in the caption of Figure 1.

EXPERIMENTAL RESULTS

A part of the theoretical results can be illustrated by the experimental behaviour of Sudan-III. Figure 9 shows the forward (reduction), backward (reoxidation) and net-components of the SWV response of Sudan-III recorded in borate buffer. As can be seen, the first redox step is a chemically reversible process, whereas the second one is totally irreversible. Being linearly dependent on pH of the medium, both SW peaks shift in the negative direction by increasing the pH. In agreement with the literature data,[11] in an aqueous medium Sudan-III undergoes successive electrode reductions of its two »azo« groups, followed by chemically reversible and irreversible protonation, in the first and second redox steps, respectively (see Scheme III)[11]:

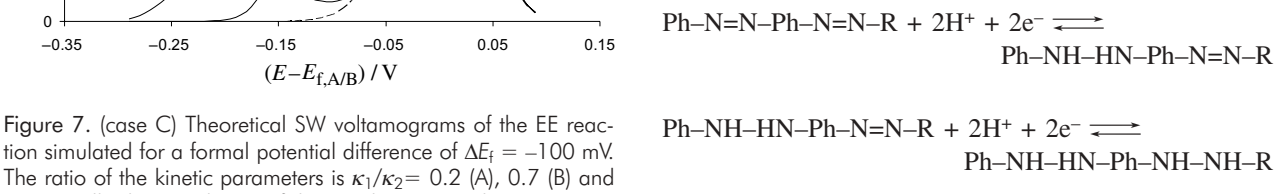

Scheme III.

where Ph and R are abbreviations for phenyl and 2-naphtol radical, respectively.

Both SWV peaks are appreciably sensitive to the accumulation time. Increasing the accumulation time caused both peaks to enhance proportionally. Moreover, after long accumulation time, *i.e.*, 120 s for 5×10^{-5} mol/l concentration of Sudan-III, a consecutive cycling of the potential did not affect significantly the heights of the peaks, which implies that all the species involved in the redox reaction are immobilised firmly on the electrode surface. This voltammetric behaviour is typical of a surface electrode reaction occurring mainly on the working electrode surface, which is the main prerequisite for the illustration of the foregoing theoretical results.

As can be seen from Figure 9, for an amplitude of E_{sw} = 25 mV and a signal frequency of f = 100 Hz, the potential separation between the two SWV peaks of Sudan-III is about 230 mV. Consequently, this is the case of a surface EE reaction in which both redox steps are separated effectively and behave as independent redox reactions (case A in Theoretical results). As the theory predicted, the kinetics of the EE mechanism consisting of two-isolated redox reactions may be inspected effectively utilising the method of »quasireversible maximum«.

Before presenting the data of the kinetic measurements of Sudan-III, it is reasonable to consider the properties of the first SW peak in more detail, since the first redox step of Sudan-III, in which an exchange of two electrons is involved, can be regarded either as a two-electron EE reaction (case B in Theoretical results), or a two-electron one-step surface reaction. As recommended in the previous section (see Case B), inspection of the half-peak width of the first SW peak of Sudan-III was carried out by varying the signal frequency (see Figure 10). The half-peak width decreases slightly with the logarithm of the inverse signal frequency, in agreement with the predictions of the theoretical results presented in Figure 6. The half-peak width of the first peak ranged from 50 to 70 mV, indicating that the reaction occurs as a simple one-step two-electron surface redox reaction (compare Figures 10 and 6). Note that the typical interval values for the half-peak width of the two-electron EE reaction ranged from 110 to 70 mV.

Inspecting the peak currents of the first SW peak over the frequency interval $10 \leq f/\text{Hz} \leq 650$, the quasireversible maximum for Sudan-III was constructed (see Figure 11). Note that the ratio between the real peak current and the signal frequency (ordinate in Figure 11) corresponds to the dimensionless peak current $\Delta\Psi_p = \Delta I_p/(nFSf\Gamma^*)$, while the inverse signal frequency $1/f$ (abscissa in Figure 11) corresponds to the kinetic parameter $\kappa = k_s/f$. The critical frequency associated with the experimental quasire-

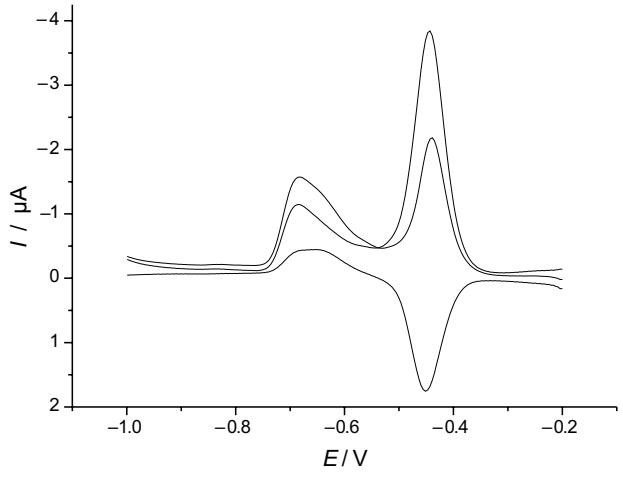

Figure 9. Square wave voltamogram of 5×10^{-5} mol/L Sudan-III solution recorded in borate buffer at pH = 10. The experimental conditions are: accumulation potential, $E_{acc.}$ = –0.2 V; accumulation time, $t_{acc.}$ = 30 s; SW amplitude, E_{sw} = 25 mV; SW frequency, f = 100 Hz and potential step, dE = 4 mV.

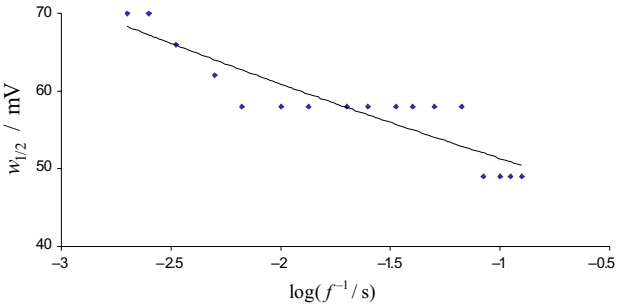

Figure 10. The dependence of the half-peak width of the first SW peak of Sudan-III on the logarithm of the inverse signal frequency. The experimental conditions were the same as in Figure 9.

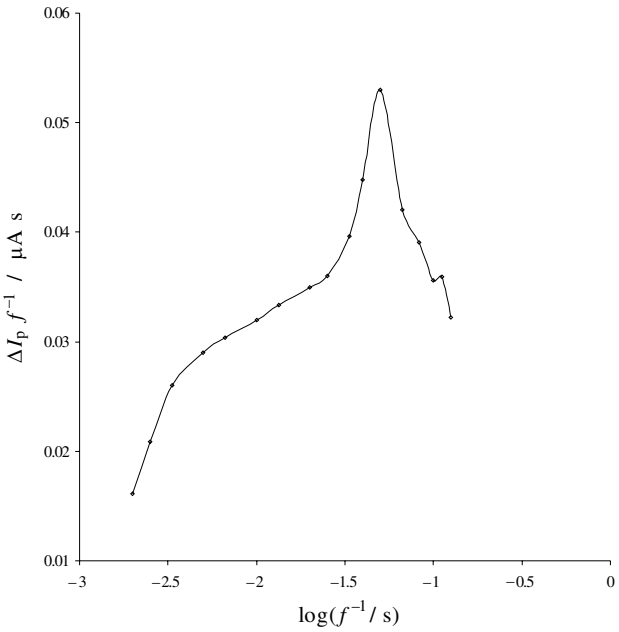

Figure 11. The quasireversible maximum of Sudan-III. The dependence of the ratio $\Delta I_p/f$ on log(1/f) for the first redox process of Sudan III. The presented data were recorded for an amplitude of E_{sw} = 20 mV. All other conditions are the same as in Figure 9.

versible maximum is f_{max} = 25 Hz. For the selected experimental conditions, the critical kinetic parameter is $\kappa_{max} = 1.18 \pm 0.05$, which applies to the transfer coefficient of $0.24 \leq \alpha \leq 0.85$.[7] Hence, the estimated value for the standard rate constant of the first redox step of Sudan-III is $k_s = 30 \pm 1$ s^{-1}.

It should be emphasised that the phenomenon of quasireversible maximum is associated with the first redox step of Sudan-III only, since the second one appears as a totally irreversible redox reaction. However, the variation of the signal frequency influences the position of the second SWV peak. As expected for an irreversible surface redox reaction, the peak potential shifts in the negative direction in proportion to the logarithm of the signal frequency. The relationship E_p-log(f) is linear with a slope of –103 mV. The theoretical slope of this dependence is $-2.303(RT/n\alpha F) \pm 0.006$ V. Therefore, the electron transfer coefficient for the second reduction step of Sudan-III is 0.29 ± 0.05. The same parameter can be calculated on the basis of the half-peak width. The theoretical half-peak width of an irreversible surface redox reaction is $w_{1/2} = 0.06/(n\alpha)$ V. Since the half-peak width of the second SW peak of Sudan-III is 105 mV (see Figure 9), the electron transfer coefficient estimated on the basis of half-peak width is 0.28, which is in good agreement with the previous value.

Finally, the effect of the signal amplitude will be discussed. For an amplitude of E_{sw} = 100 mV and frequency f = 30 Hz, the response consists of three SW peaks. This is a consequence of the splitting of the first SWV peak of Sudan-III. Only the first SW peak is subject to splitting. The second SW peak does not split since it is ascribed to an irreversible redox process. For amplitudes higher than 100 mV, the potential separation between split SW peaks increases, which causes overlapping with the response of the irreversible process. The influence of the signal amplitude is in agreement with the theoretical predictions presented in Figure 3. However, the shape of the voltammetric response of Sudan-III at a large signal amplitude is rather complex, indicating that the variation of the amplitude will not provide useful information about the kinetics of the redox system under study.

Acknowledgments. – V. Mirčeski thanks A. V. Humboldt-Stiftung for a Humboldt fellowship; R. Gulaboski thanks Deutscher Akademische Austauschdienst (DAAD) for a PhD scholarship.

APPENDIX

It is instructive to investigate the variation of the charging current in the course of a single SW potential pulse for a simple surface redox reaction (II), since it is frequently claimed that SWV is discriminative against the charging current only in the case of diffusion controlled processes. The aim of the following brief analysis is to check the ability of SWV to avoid the charging current when the electrode is covered by an electroactive film.

The interfacial potential distribution and the capacitance of an electrode covered by an electroactive film are treated by Smith and White.[35] The total capacitance C_T of the interface is defined as:

$$C_T^{-1} = C_1^{-1} + C_{dif}^{-1}\left[1 + \frac{n^2F^2\Gamma^*}{RTC_1}\Theta(1-\Theta)\right]$$

Here, C_1 is the capacitance of the adsorbed film, C_{dif} is the capacitance of the solution, and $\Theta = \Gamma(A)/\Gamma^*$ is the relative surface coverage. All other symbols have the same meaning as in the section Mathematical model. Obviously, the total capacitance is a complex function of the surface concentration of the oxidised form of the adsorbate Γ(A). It means that the faradic current affects the charging current in the course of the potential pulse by varying the surface concentration Γ(A).

In general, in a single potential pulse experiment, the charging current changes with time according to the following equation:

$$I_c = \frac{E}{R_s}\exp\left(-\frac{\tau}{R_s C_T S}\right)$$

Here, I_c is the charging current, E is the relative potential with respect to the potential of zero charge E_{pzc}, and R_s is the solution resistance.

To estimate the charging current, and to compare it with the faradaic current, we will use the same parameters as in the example given by Smith,[35] *i. e.*, C_1 = 0.035 F m^{-2}, C_{dif} = 2.278 F m^{-2}, E *vs.* E_{PZC} = 0.5 V, $\Gamma^* = 1 \times 10^{-10}$ mol cm^{-2}, R_s = 40 Ω, n = 1, and S = 0.09 cm^2. To calculate faradaic current,[10] we set the following conditions: f = 2000 Hz (it corresponds to the duration of a single potential pulse of τ = 0.25 ms), standard rate constant of k_s = 20 000 s^{-1} (reversible reaction, $\log(k_s/f) = 1$), and E *vs.* $E^0 = 0$. The calculations show that after 0.1 ms, the charging current decreases to 0.5 % of its initial value. At the same moment, the ratio of the faradaic I_f and charging I_c current is I_f/I_c = 64.9. Moreover, at the end of the pulse, when the current is actually measured in SWV, the charging current decreases to (3.7×10^{-7}) % of its initial value and the ratio is $I_f/I_c = 2.1 \times 10^4$.

It is particularly important to investigate the ratio of the faradic and charging currents under the conditions when the quasireversible maximum is reached. The critical value of the kinetic parameter $(k_s/f)_{max}$ associated with the quasireversible maximum is close to 1[7], which means that the highest faradaic current is measured when the duration of the potential pulse is synchronised to the rate of the electron transfer *i.e.*, $f \approx k_s$. For instance, if $k_s = f$ = 2000 s^{-1}, and all other conditions are the same as in the previous

example, the ratio of the faradaic and charging currents at the end of the pulse is $I_f/I_c = 1.67 \times 10^7$, which shows clearly that the current measured is virtually completely due to the faradaic reaction. It is important to note that under these conditions the charging current measured at the very beginning of the pulse is larger than the faradaic current, indicating that there are great advantages of measuring the current after a certain time of potential pulse application. Therefore, it is quite clear that SWV can effectively discriminate against the charging current even in the case of the surface redox reaction.

REFERENCES

1. A. Webber, M. Shah, and J. Osteryoung, *Anal. Chim. Acta* **157** (1984) 1–16.
2. A. Webber and J. Osteryoung, *Anal. Chim. Acta* **157** (1984) 17–29.
3. Š. Komorsky-Lovrić and M. Lovrić, *Electroanalysis* **6** (1994) 651–656.
4. M. Lovrić, Š. Komorsky-Lovrić, and R. W. Murray, *Electrochim. Acta* **33** (1988) 739–744.
5. M. Lovrić and Š. Komorsky-Lovrić, *J. Electroanal. Chem.* **248** (1988) 239–253.
6. J. J. O'Dea, A. Ribes, and J. Osteryoung, *J. Electroanal. Chem.* **345** (1993) 287–301.
7. Š. Komorsky-Lovrić and M. Lovrić, *J. Electroanal. Chem.* **384** (1995) 115–122.
8. Š. Komorsky-Lovrić and M. Lovrić, *Anal. Chim. Acta* **305** (1995) 248–255.
9. R. Gulaboski, V. Mirčeski, and Š. Komorsky-Lovrić, *Electroanalysis* **14** (2002) 355–364.
10. V. Mirčeski and M. Lovrić, *Electroanalysis* **9** (1997) 1283––1287.
11. T. M. Florence, *J. Electroanal. Chem*. **52** (1974) 115–132.
12. J. J. O'Dea and J. Osteryoung, *Anal. Chem*. **69** (1997) 650––658.
13. V. Mirčeski and M. Lovrić, *Croat. Chem. Acta* **73** (2000) 305–329.
14. M. M. Baizer and H. Lund, *Organic Electrochemistry*, Marcel Dekker, New York, 1983.
15. A. J. Bard and H. Lund, *Encyclopaedia of Electrochemistry of the Elements*, Marcel Dekker, New York, 1979.
16. R. Meunier-Prest and E. Laviron, *J. Electroanal. Chem.* **410** (1996) 133–143.
17. J. Osteryoung and M. Schriener, *Anal. Chem.* **19** (1988) S7.
18. J. Osteryoung and J. J. O'Dea, in: A. J. Bard (Ed.) *Electroanalytical Chemistry, A Series of Advances,* Vol. 14, Marcel Dekker, New York, 1987.
19. A. B. Miles and R. G. Compton, *J. Electroanal. Chem.* **499** (2001) 1–16.
20. A. B. Miles and R. G. Compton, *J. Electroanal. Chem*. **499** (2000) 75–89.
21. A. B. Miles and R. G. Compton, *J. Phys. Chem. B* **104** (2000) 5331–5342.
22. V. Mirčeski and R. Gulaboski, *Electroanalysis* **13** (2001) 1326–1334.
23. V. Mirčeski, *J. Electroanal. Chem*. **508** (2001) 138–149.
24. V. Mirčeski, R. Gulaboski, B. Jordanoski, and S. Komorsky-Lovrić, *J. Electroanal. Chem*. **490** (2000) 37–47.
25. V. Mirčeski, M. Lovrić and R. Gulaboski, *J. Electroanal. Chem.* **515** (2001) 91–100.
26. V. Mirčeski and R. Gulaboski, *Microchim. Acta* **138** (2002) 33–42.
27. J. Hirst and F. A. Armstrong, *Anal. Chem*. **70** (1998) 5062––5071.
28. F. A. Armstrong, H. A. Heering, and J. Hirst, *Chem. Soc. Rev.* **26** (1997) 169–179.
29. J. Hirst, G. N. L. Jameson, J. W. A. Allen, and F. A. Armstrong, *J. Am. Chem. Soc*. **120** (1998) 11994–11999.
30. J. Hirst, J. L. C. Duff, G. N. L. Jameson, M. A. Kemper, B. K. Burgess, and F. A. Armstrong, *J. Am. Chem. Soc.* **120** (1998) 7085–7094.
31. F. A. Armstrong and G. S. Wilson, *Electrochim. Acta* **45** (2000) 2623–2645.
32. R. S. Nicholson and M. L. Olmstead, in: J. S. Mattson, H. B. Mark, and H. C. MacDonald (Eds.), *Electrochemistry, Calculations, Simulation and Instrumentation,* Vol. 2, Marcel Dekker, New York, 1972, pp. 120–137.
33. A. J. Bard and L. R. Faulkner, *Electrochemical Methods, Fundamentals and Applications,* John Wiley & Sons, New York, 1980, pp. 232–236.
34. E. Laviron, *J. Electroanal. Chem*. **101** (1979) 19–28.
35. C. P. Smith and H. S. White, *Anal. Chem.* **64** (1992) 2398––2405.

SAŽETAK

Teorijsko i eksperimentalno istraživanje dvostupanjske kvazireverzibilne površinske redoks-reakcije pravokutnovalnom voltammetrijom

Valentin Mirčeski i Rubin Gulaboski

Opisan je prošireni teorijski pristup dvostupanjskoj površinskoj redoks-reakciji (EE) pod uvjetima pravokutnovalne voltammetrije. Općim teorijskim modelom obuhvaćene su EE reakcije različitih stupnjeva reverzibilnosti pojedinih elektronskih prijelaza. Integralne jednadžbe koje čine matematički model riješene su numerički. Prividna reverzibilnost pojedinih stupnjeva EE reakcije ovisi o bezdimenzijskim kinetičkim parametrima

$\kappa_1 = k_{s,1} / f$ i $\kappa_2 = k_{s,2} / f$, pri čemu su $k_{s,1}$ i $k_{s,2}$ standardne konstante brzina prvog i drugog elektronskog prijelaza, a f je frekvencija voltammetrijske pobude. Odziv EE reakcije može biti samo jedan voltammetrijski val ili se javljaju dva odvojena vala, što prvenstveno zavisi o razlici formalnih (standardnih) potencijala pojedinih stupnjeva reakcije i o omjeru kinetičkih parametara κ_1 i κ_2. Raspravlja se i o utjecaju koeficijenata pojedinih elektronskih prijelaza na oblik odziva EE reakcije. Dio teorijskih predviđanja potvrđen je kvalitativnom usporedbom s voltamogramima azo-boje Sudan-III.